

Electronic Supplementary Material (ESI) for Chem Comm.

This journal is © The Royal Society of Chemistry 2015

Electronic Supplementary Information for

A novel electron-acceptor moiety as a building block for efficient donor-acceptor based fluorescent organic light-emitting diodes

Miao-Miao Xue, Chen-Chao Huang, Yi Yuan, Ye-Xin Zhang, Man-Keung Fung* and
Liang-Sheng Liao*

Jiangsu Key Laboratory for Carbon-Based Functional Materials & Devices, Institute of
Functional Nano & Soft Materials (FUNSOM), Soochow University Suzhou, Jiangsu
215123, China.

Email: lsiao@suda.edu.cn (Prof.); mkfung@suda.edu.cn (Prof.).

Scheme S1. Synthetic routes of TPA-BFPz.

Fig. S1. TGA curve of TPA-BFPz, inset: DSC curve of TPA-BFPz.

Fig. S2. UV-Vis curves of TPA-BFPz in different solvents.

Fig. S3. Transient PL of TPA-BFPz in film.

Fig. S4. HOMO-LUMO spatial distribution of TPA-BFPz.

Fig. S5. UPS spectrum of TPA-BFPz.

Fig. S6. Energy level diagram

Fig. S7. EL spectra of devices.

Fig. S8. PE-L curves of devices.

Table S1. Photophysical, thermal properties and HOMO/LUMO energy levels of TPA-BFPz

Table S2. Photophysical properties in different solvents

Experimental Section

Characterization: ^1H NMR and ^{13}C NMR spectra were measured using a Varian Unity Inova 400 spectrometer at room temperature. Mass spectra were obtained by a Thermo ISQ mass spectrometer equipped with a direct exposure probe. UV-Vis absorption spectra were recorded by a Perkin Elmer Lambda 750 spectrophotometer. PL spectra and phosphorescent spectra were measured by a Hitachi F-4600 fluorescence spectrophotometer. Differential scanning calorimetry (DSC) was determined on a TA DSC 2010 unit at a heating rate of $10\text{ }^\circ\text{C}/\text{min}$ under nitrogen from $25\text{ }^\circ\text{C}$ to $120\text{ }^\circ\text{C}$. The glass transition temperatures (T_g) were measured from the second heating scan. Thermo gravimetric analysis (TGA) was performed on a TA SDT 2960 instrument at a heating rate of $10\text{ }^\circ\text{C}/\text{min}$ from $25\text{ }^\circ\text{C}$ to $550\text{ }^\circ\text{C}$ under nitrogen. Temperature at a 5% weight loss was used as the decomposition temperature (T_d). The ultraviolet photoemission spectroscopy (UPS) characterization was conducted in a Kratos AXIS UltraDLD ultrahigh vacuum (UHV) analysis system.

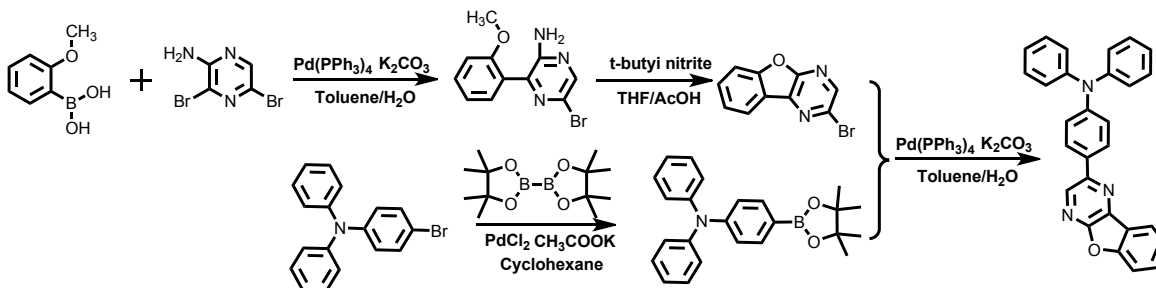
Computational methodology: The geometrical and electronic properties of TPA-BFPz were performed by the Gaussian 09 program package. The molecular structure was optimized by b3lyp (Becke three parameters hybrid functional with Lee-Yang-Perdew correlation functionals) with the 6-31G(d) atomic basis set. Molecular orbitals were visualized by Gaussview.

Device fabrication and measurements: The structure of non-doped device is ITO/HAT-CN (10 nm)/TAPC (40 nm)/TPA-BFPz (20 nm)/TmPyPB (45 nm)/Liq (2 nm)/Al, in which HAT-CN and Liq act as a hole-injection layer (HIL) and electron-injection layer (EIL), respectively. TAPC was used as a hole-transporting layer (HTL) and electron-blocking layer (EBL); TmPyPB serves as an electron-transporting layer (ETL) as well as hole-blocking layer (HBL); and Al acts as a cathode. The structure of doped device is ITO/HAT-CN (10 nm)/TAPC (40 nm)/DPEPO: TPA-BFPz (X wt%, 20 nm)/TmPyPB (45 nm)/Liq (2 nm)/Al, in which DPEPO serves as host material and X represents doping concentration of TPA-BFPz in DPEPO.

The OLEDs were all fabricated with vacuum deposition at ca. 2×10^{-6} Torr. Commercially available ITO-coated glass with a sheet resistance of ca. $30\ \Omega$ per square was used as substrates. The

ITO surface was cleaned sequentially with acetone, ethanol, and deionizer water, dried in an oven, and exposed to UV-ozone for 20 minutes. HAT-CN and Liq were deposited at a rate of 0.2-0.3 Å/s, and other organic layers were deposited at 2-3 Å/s, finally the Al electrode was deposited (ca. 5 Å/s) through a shadow mask without breaking the vacuum. All devices have an emitting area of 0.09 cm². The EL spectra, CIE coordinates and *J-V* curves of the devices were measured with a PHOTO RESEARCH Spectra Scan PR 655 photometer and a KEITHLEY 2400 Source Meter constant current source at room temperature. The EQE values were done by calculation.

Preparation of compounds: All raw materials and reagents were purchased from commercial sources and used as received without further purification. Solvents for chemical synthesis were purified according to the standard procedures.



Scheme S1. Synthetic routes of TPA-BFPz

Synthesis of 5-bromo-3-(2-methoxyphenyl)pyrazin-2-amine: A mixture of (2-methoxyphenyl)boronic acid (5.0 g, 32.9 mmol), 3,5-dibromopyrazin-2-amine (8.3 g, 32.9 mmol), potassium carbonate (13.6g, 98.7 mmol), toluene (250 mL) and distilled water (40 mL), tetrakis(triphenylphosphine)palladium(0) (1.7 g, 1.6 mmol) was heated at refluxed under N₂ for 48 h. The reaction mixture was cooled to room temperature, and extracted with ethyl acetate and distilled water. The organic layer was dried over anhydrous magnesium sulfate and evaporated in vacuo to give the crude product, which was purified by column chromatography on silica gel using hexane/ethyl acetate gradient mixture as eluent, providing 5.5 g of 5-bromo-3-(2-methoxyphenyl)pyrazin-2-amine.

Yield 60%; C₁₁H₁₀BrN₃O; MS (EI) *m/z* 280.98 [(M+H)⁺]. ¹H NMR (600 MHz, CDCl₃, δ); 8.09 (s, 1H), 7.44-7.40 (m, 2H), 7.09 (t, 1H, *J*=6.0 Hz), 7.00 (d, 1H, *J*=12.0 Hz), 4.68 (s, 2H), 3.84 (s, 3H); ¹³C NMR (600 MHz, CDCl₃, δ); 156.43, 152.23, 142.97, 139.84, 131.82, 131.07, 126.46, 124.91, 121.67, 111.39, 55.78.

Synthesis of 2-bromobenzofuro[2,3-b]pyrazine (2-Br-BFPz): 5-bromo-3-(2-methoxyphenyl)pyrazin-2-amine (4.5 g, 16.1 mmol) in tetrahydrofuran (20 mL) and glacial acetic acid (40 ml) were stirred at -10 °C and *tert*-butyl nitrite (6.6 g, 49.7 mmol) was added via syringe over a period of 15 min. After stirring for 1.5h at -10 °C, the reaction mixture was stirred at 0 °C over a period of 12 h. The reaction mixture was warmed to room temperature, diluted with 80 mL of distilled water. Solid material was filtered and dried, providing 1.8g of pure 2-bromobenzofuro[2,3-b]pyrazine (2-Br-BFPz).

Yield 45%; C₁₀H₅BrN₂O; MS (EI) *m/z* 248.04 [(M+H)⁺]. ¹H NMR (600 MHz, CDCl₃, δ); 8.46 (s, 1H), 8.22 (d, 1H, *J*=6.0 Hz), 7.69 (d, 2H, *J*=6.0), 7.52-7.49 (m, 1H); ¹³C NMR (600 MHz, CDCl₃, δ); 156.93, 141.56, 131.45, 124.74, 122.39, 120.60, 112.85;

Synthesis of 4-(benzofuro[2,3-b]pyrazin-2-yl)-N,N-diphenylaniline (TPA-BFPz): N,N-diphenyl-4-(4,4,5,5-tetramethyl-1,3,2-dioxaborolan-2-yl)aniline was prepared according to the literature.⁽¹⁾ A mixture of 2-bromobenzofuro[2,3-b]pyrazine (2-Br-BFPz, 1.2 g, 4.84 mmol), N,N-diphenyl-4-(4,4,5,5-tetramethyl-1,3,2-dioxaborolan-2-yl)aniline (2.69 g, 7.26 mmol), potassium phosphate tribasic (3.0 g, 14.5 mmol), tetrakis(triphenylphosphine)palladium(0) (0.3 g, 1.6 mmol), toluene (120 ml) and distilled water (12 ml) was refluxed under N₂ for 48 h. Then reaction mixture was cooled down to room temperature, diluted with 50 mL water and extracted with ethyl acetate. The organic extracts were dried over anhydrous magnesium sulfate, filtered, and evaporated. The crude material was purified by column chromatography on silica gel using dichloromethane/n-hexane as eluent. Additional purification by sublimation resulted in 1.2g of pure blue-green compound (TPA-BFPz).

Yield 60%; C₂₈H₁₉N₃O; MS (EI) *m/z* 413.25 [(M+H)⁺]. ¹H NMR (400 MHz, CDCl₃, δ); 8.79 (s, 1H), 8.35 (d, 1H *J*=8.0), 8.01 (d, 2H, *J*=8.0), 7.73-7.70 (m, 2H), 7.56-7.54 (m, 1H), 7.35-7.32 (m, 4H), 7.27-7.21 (m, 6H), 7.13 (t, 2H, *J*=4.0 Hz); ¹³C NMR (400 MHz, CDCl₃, δ); 156.29, 155.70, 149.07, 148.60, 146.83, 136.65, 136.52, 130.06, 129.78, 128.92, 127.47, 124.45, 123.72, 122.68, 121.71, 121.45, 112.22.

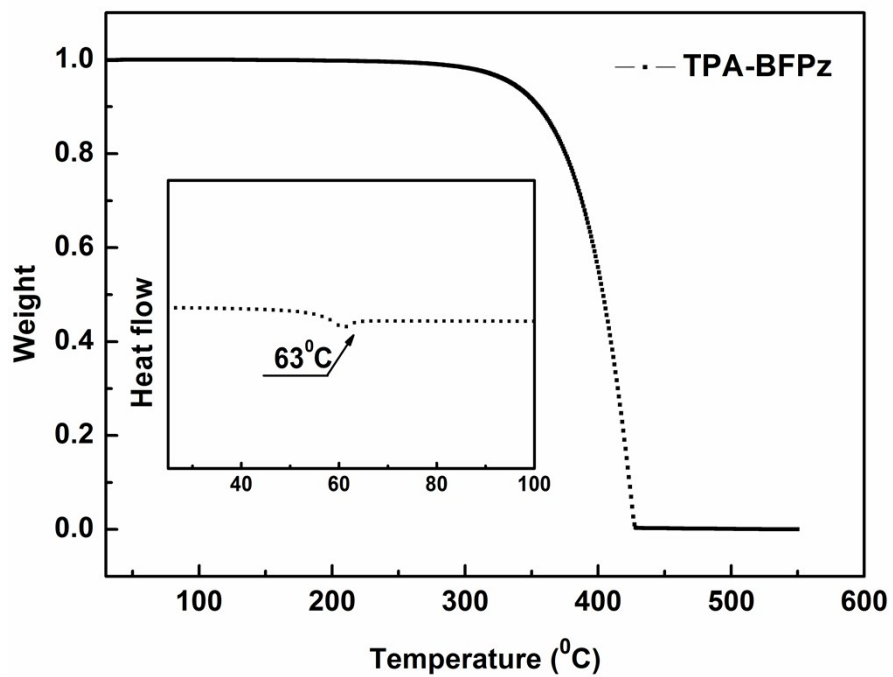


Fig. S1. TGA curve of TPA-BFPz, inset: DSC curve of TPA-BFPz.

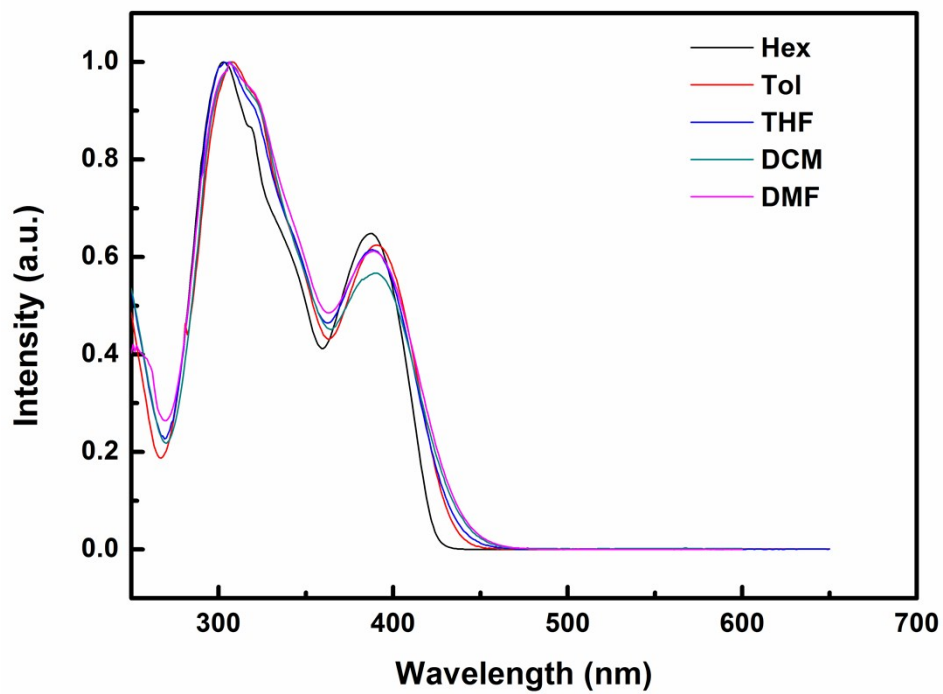


Fig. S2. UV-Vis curves of TPA-BFPz in different solvents

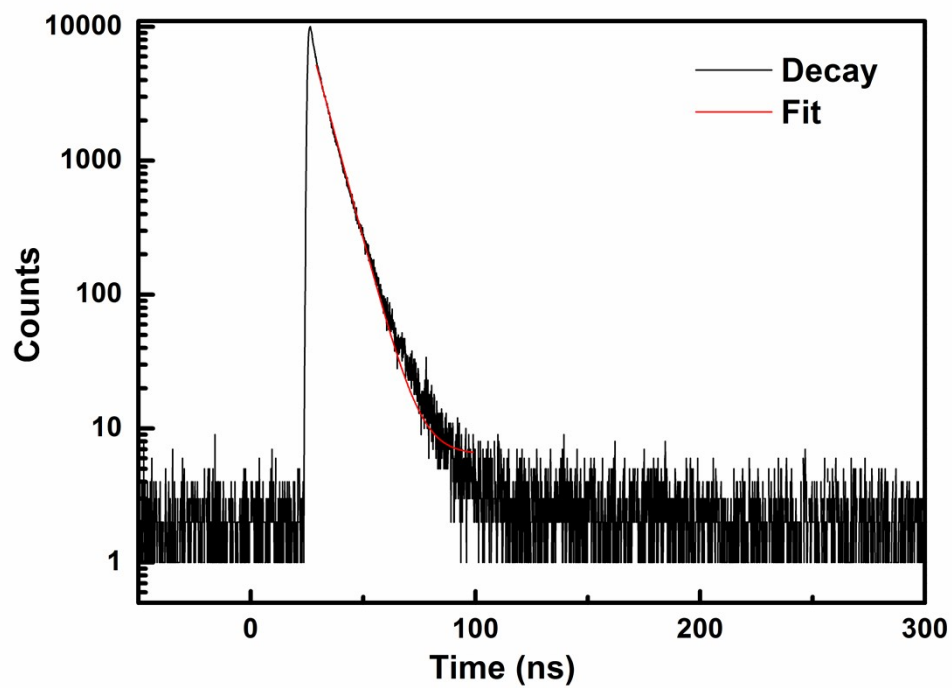


Fig. S3. Transient PL of TPA-BFPz in film

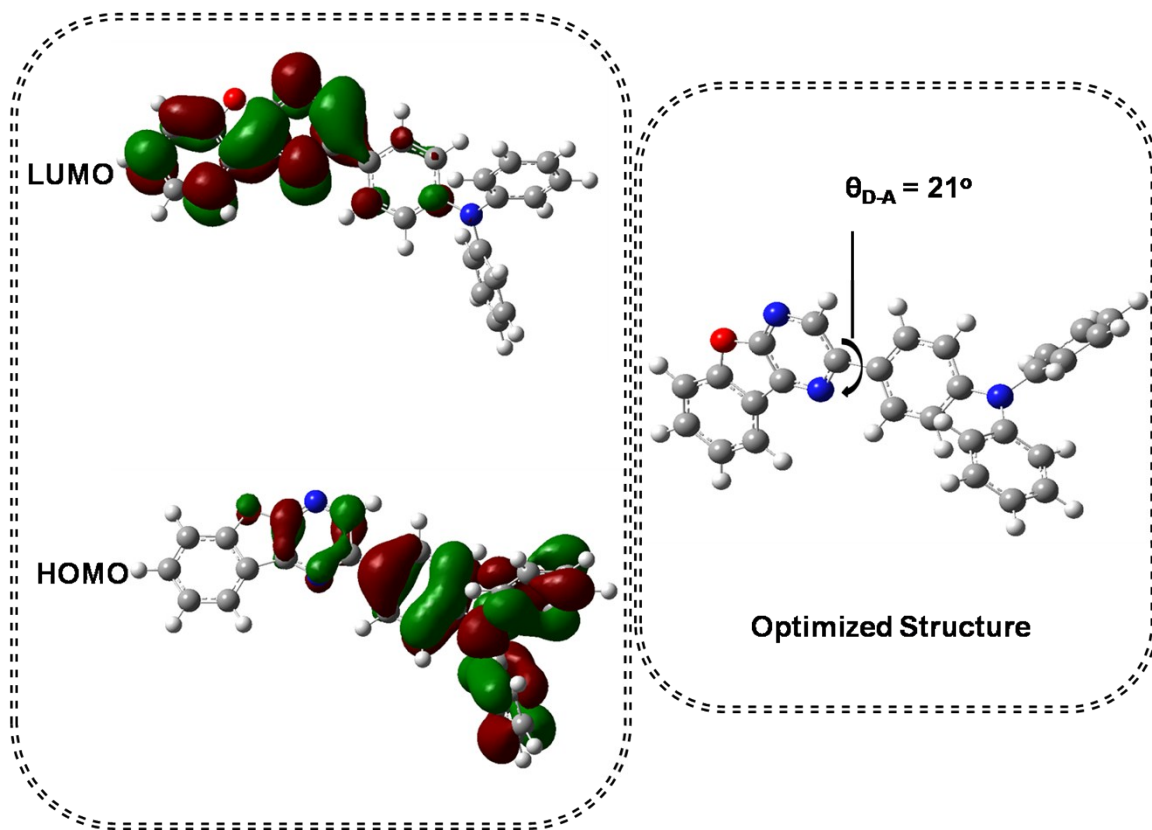


Fig. S4. HOMO/LUMO spatial distribution of TPA-BFPz

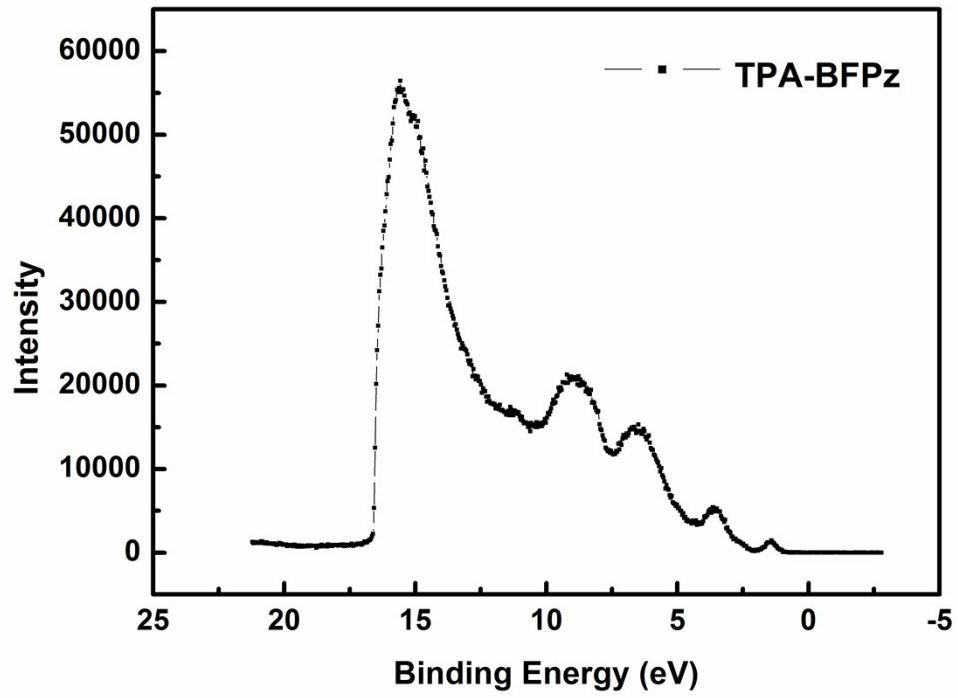


Fig. S5. UPS curve of TPA-BFPz

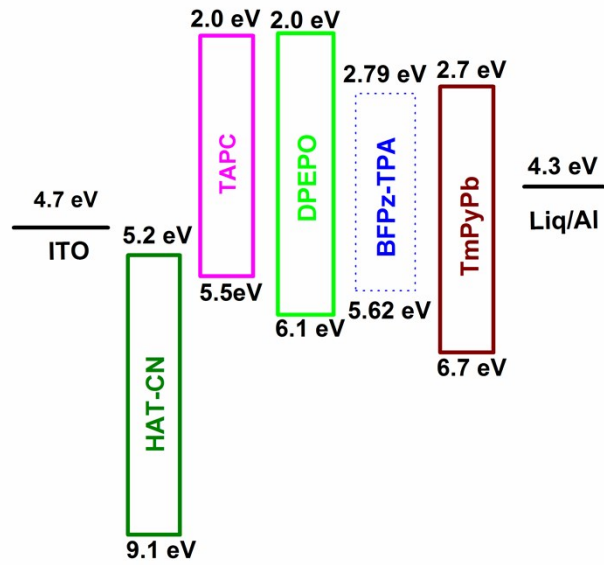


Fig. S6. Energy level diagram

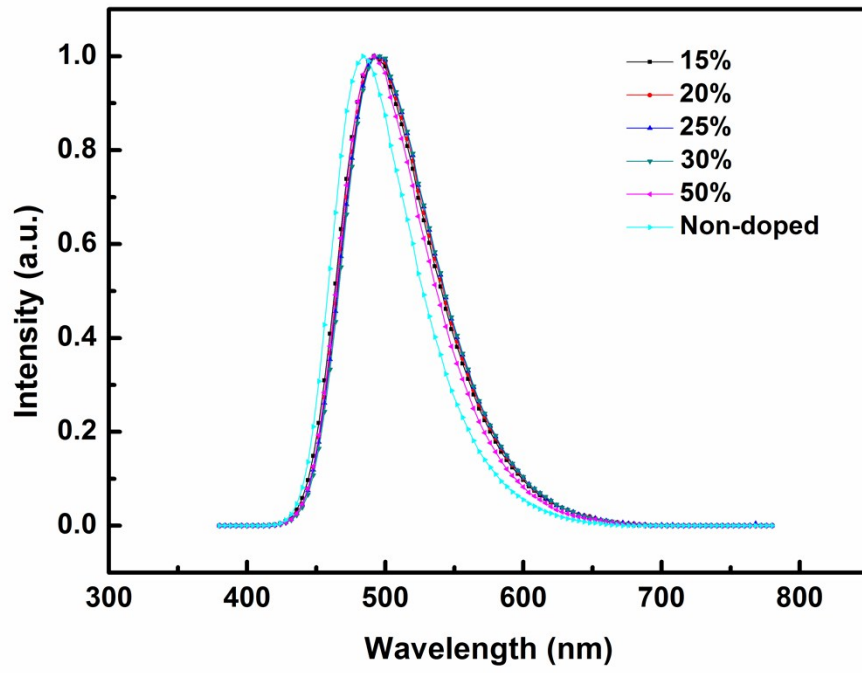


Fig. S7. EL spectra of devices

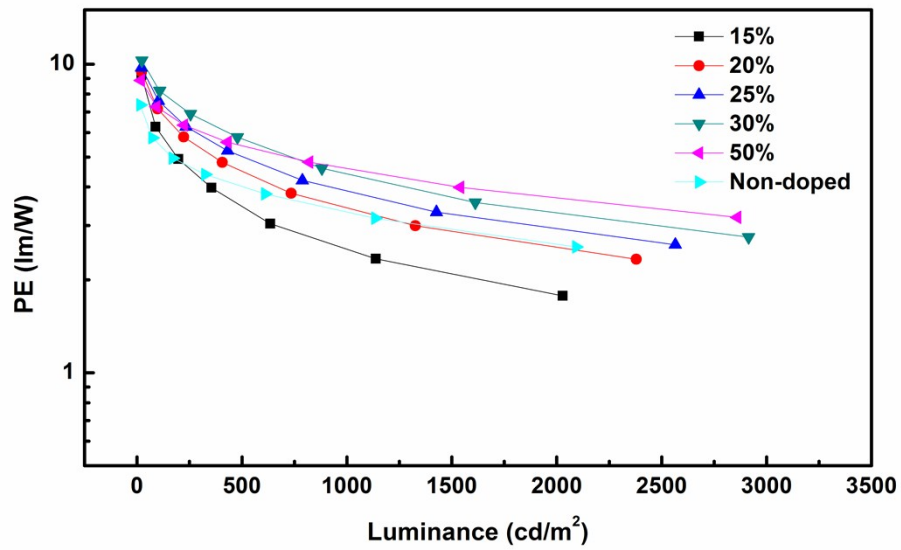


Fig. S8. PE-L curves of devices.

Table S1. Photophysical, thermal properties and HOMO/LUMO energy levels of TPA-BFPz

	Abs ^a	PL ^b	T_g ^c	T_d ^d	E_g ^e	HOMO ^f	LUMO ^g
	[nm]	[nm]	[°C]	[°C]	[eV]	[eV]	[eV]
TPA-BFPz	308, 394	482	63	350	2.83	5.62	2.79

^aMeasured in toluene solution at room temperature. ^bMeasured in film at room temperature. ^c T_g : Glass transition temperature. ^d T_d : Decomposition temperature. ^e E_g : Band gap energy was calculated from the corresponding absorption onset in toluene solution. ^fHOMO energy level was calculated from UPS data. ^gLUMO energy level was calculated from the HOMO and E_g .

Table S2. Photophysical properties in different solvents

Solvent	PL (nm)
Hex	428
Tol	466
THF	506
DCM	543
DMF	563

Reference

- (1) Y. M. Zhang, F. Y. Meng, J. H. Tang, Y. F. Wang, C. F. You, H. Tan, Y. Liu, Y. W. Zhong, S. J. Su W. G. Zhu, *Dalton Trans.*, 2016, **45**, 5071.